

UC Davis

UC Davis Previously Published Works

Title

Injectable mineralized microsphere-loaded composite hydrogels for bone repair in a sheep bone defect model

Permalink

<https://escholarship.org/uc/item/7350t4gp>

Authors

Ingavle, Ganesh C
Gionet-Gonzales, Marissa
Vorwald, Charlotte E
et al.

Publication Date

2019-03-01

DOI

10.1016/j.biomaterials.2019.01.005

Peer reviewed



Published in final edited form as:

Biomaterials. 2019 March ; 197: 119–128. doi:10.1016/j.biomaterials.2019.01.005.

Injectable mineralized microsphere-loaded composite hydrogels for bone repair in a sheep bone defect model

Ganesh C. Ingavle^{#1,4}, Marissa Gionet-Gonzales^{#1}, Charlotte E. Vorwald¹, Laurie K. Bohannon², Kaitlin Clark², Larry D. Galuppo², and J. Kent Leach^{1,3}

¹Department of Biomedical Engineering, University of California, Davis, Davis, CA 95616

²Department of Surgical & Radiological Sciences, UC Davis School of Veterinary Medicine, Davis, CA 95616

³Department of Orthopaedic Surgery, School of Medicine, UC Davis Health, Sacramento, CA 95817

⁴Symbiosis Center for Stem Cell Research, Symbiosis International University, Pune-412115, India

These authors contributed equally to this work.

Abstract

The efficacy of cell-based therapies as an alternative to autologous bone grafts requires biomaterials to localize cells at the defect and drive osteogenic differentiation. Hydrogels are ideal cell delivery vehicles that can provide instructional cues *via* their composition or mechanical properties but commonly lack osteoconductive components that nucleate mineral. To address this challenge, we entrapped mesenchymal stromal cells (MSCs) in a composite hydrogel based on two naturally-derived polymers (alginate and hyaluronate) containing biomineralized polymeric microspheres. Mechanical properties of the hydrogels were dependent upon composition. The presentation of the adhesive tripeptide Arginine-Glycine-Aspartic Acid (RGD) from both polymers induced greater osteogenic differentiation of ovine MSCs *in vitro* compared to gels formed of RGD-alginate or RGD-alginate/hyaluronate alone. We then evaluated the capacity of this construct to stimulate bone healing when transplanting autologous, culture-expanded MSCs into a surgical induced, critical-sized ovine iliac crest bone defect. At 12 weeks post-implantation, defects treated with MSCs transplanted in composite gels exhibited significant increases in blood

Corresponding author: J. Kent Leach, Ph.D., University of California, Davis, Department of Biomedical Engineering, 451 Health Sciences Drive, Davis, CA 95616, Phone: (530) 754-9149, jkleach@ucdavis.edu.
CrediT Author Statement

Ganesh Ingavle: Conceptualization, Formal analysis, Methodology, Investigation, Writing – original draft, Writing – review & editing

Marissa Gionet-Gonzales: Investigation, Formal analysis, Methodology, Visualization, Writing – review & editing

Charlotte Vorwald: Investigation, Formal analysis, Visualization, Writing – review & editing

Laurie Bohannon: Investigation

Kaitlin Clark: Investigation

Larry Galuppo: Funding acquisition, Methodology, Investigation, Supervision

Kent Leach: Conceptualization, Formal analysis, Funding acquisition, Methodology, Supervision, Project administration, Writing – original draft, Writing – review & editing

Conflict of Interest: All authors declare that they have no conflict of interest.

8. DATA AVAILABILITY

The processed data required to reproduce these findings are available to download from <http://dx.doi.org/10.17632/67r4m4m8h4.1>

vessel density, osteoid formation, and bone formation compared to acellular gels or untreated defects. These findings demonstrate the capacity of osteoconductive hydrogels to promote bone formation with autologous MSCs in a large animal bone defect model and provide a promising vehicle for cell-based therapies of bone healing.

Keywords

alginate; hyaluronate; biomineralization; hydrogel; osteogenesis; osteoconductive

1. INTRODUCTION

Cell-based therapies are an exciting strategy to stimulate bone healing in large bone defects resulting from trauma, disease, or malformation. The transplantation of mesenchymal stromal cells (MSCs), adult-derived progenitor cells commonly derived from bone marrow or other tissue compartments, increases bone volume in multiple defect models.[1] However, the effectiveness of this approach requires the transplantation of MSCs using a biomaterial to localize cells at the defect, limit migration away from the target site, and potentially include instructional signals to drive cellular behavior.[2]

Hydrogels have attracted intense interest as a cell carrier because of their tailorability and potential for minimally invasive administration to the defect site.[3,4] Alginate is broadly used in forming hydrogels due to its chemically-controlled material properties and presentation of specific cues that regulate cell adhesion and phenotype.[2,5] The tripeptide Arginine-Glycine-Aspartic Acid (RGD) is widely employed to engage integrins by mimicking the adhesive binding properties of matricellular proteins such as fibronectin.[6] Hyaluronate is another promising platform in tissue engineering due to its intrinsic viscosity, engagement with cells through CD44-specific interactions, and tunability.[7] Beyond its use as a cell carrier, hyaluronate is under investigation as a biomacromolecule to stimulate repair of connective tissues, making it a promising adjuvant for local delivery.[8] These two polymers were previously combined to form composite hydrogels for cartilage regeneration, capitalizing on the CD44 expression of chondrocytes to address their limited engagement and impaired responsiveness to RGD.[9,10] The inclusion of hyaluronate enabled cell-mediated crosslinking within the composite gels that was not observed with RGD-modified alginate alone.

Hydrogels provide an ideal platform to efficiently entrap cells for delivery to the defect site, yet these materials generally lack sufficient osteoconductivity to nucleate calcium, integrate with surrounding bone, and promote bone formation. Carbonated apatite coatings exhibiting characteristics similar to native bone have been applied to various materials to enhance osteoconductivity and contribute to bone repair.[11–13] We previously demonstrated the potential to enhance the osteoconductivity of fibrin hydrogels by supplementation with mineralized poly(lactide-co-glycolide) (PLG) microspheres, resulting in significant increases in bone mineral density over non-mineralized gels when implanted in a rodent calvarial defect.[14] Polymeric microspheres are less dense than other bioceramics (*e.g.*, β -tricalcium phosphate, hydroxyapatite), thus allowing for more homogenous distribution throughout the

gel and improved spatial interaction with entrapped cells. However, these osteoconductive gels were not transplanted with bone-forming cells, resulting in relatively low quantities of new bone and motivating a critical need to evaluate this approach for stimulating bone repair using MSCs.

We hypothesized that the transplantation of autologous MSCs within peptide-modified composite hydrogels containing mineralized polymeric microspheres would enhance hydrogel osteoconductivity, increase its osteogenic potential, and promote bone healing in a large animal bone defect model. We further hypothesized that the inclusion of hyaluronate would enhance osteogenesis due to its promise in stimulating repair of connective tissues. We characterized the physical properties of these composite gels and the osteogenic response of ovine MSCs *in vitro*. We then examined the ability of composite hydrogels transplanting autologous MSCs to promote repair of critical-sized iliac crest bone defects using an ovine model.

2. MATERIALS AND METHODS

2.1. Isolation and culture of ovine MSCs

Treatment of experimental animals was in accordance with the UC Davis animal care guidelines and all National Institutes of Health animal handling procedures. Bone marrow collection from 12 adult female Swiss Alpine sheep (approximately 60–80 kg) was performed under general anesthesia. After aseptic preparation and draping of the sternum, a 13.5-gauge 2.5-inch bone marrow aspiration needle was inserted through the skin into the medullary cavity of a sternebra, and bone marrow aspirate (40–60 mL total volume) was collected into a heparinized 60 mL syringe (Supplementary Fig. 1A). Animals were returned to small pens during stem cell isolation and expansion (approximately 3 weeks). After removal of plasma and red blood cells, cells were passaged at a low density into successively larger tissue culture flasks with culture media comprised of α -MEM supplemented with 10% fetal bovine serum (JR Scientific, Woodland, CA), 1% penicillin/streptomycin and 0.1% fungizone (Mediatech, Manassas, VA). Medium was replaced every 2–3 days to achieve an adherent cell population with fibroblastic morphology. Cells were used at passage 3–4.

To validate that the recovered cells were indeed MSCs, we performed flow cytometry for known MSC surface markers (CD90, CD105, CD44, CD45) and characterized their trilineage potential (*i.e.*, osteogenesis, chondrogenesis, adipogenesis) in monolayer culture using lineage-specific media for up to 3 weeks.[15,16] Characterization and all *in vitro* studies were performed with MSCs from a single donor.

2.2. Fabrication of apatite-coated PLG microspheres

Poly(lactide-*co*-glycolide) (PLG) microspheres were formed from PLG pellets (85:15 DLG 7E; Lakeshore Biomaterials, Birmingham, AL) using a standard double-emulsion process and lyophilized to form a free-flowing powder.[14] Microspheres were hydrolyzed for 10 min in 0.5 M NaOH to functionalize the polymer surface and then rinsed in distilled H₂O. Modified simulated body fluid (mSBF) was prepared as previously described[17] and

consisted of the following reagents dissolved in distilled H₂O: 141 mM NaCl, 5.0 mM CaCl₂, 4.2 mM NaHCO₃, 4.0 mM KCl, 2.0 mM KH₂PO₄, 1.0 mM MgCl₂, and 0.5 mM MgSO₄. The solution was held at pH 6.8 to avoid homogeneous precipitation of CaP phases. Microspheres were placed in mSBF and incubated at 37°C for 7 days, making sure to exchange the solution daily to maintain appropriate ion concentrations, frozen overnight at -80°C, and lyophilized for 3 days. Microparticles possessed diameters in the range of 50–100 μm as previously reported.[14,18] Microspheres were sterilized under ultraviolet light for 16–18 hours prior to use.

2.3. Preparation and seeding of composite hydrogels

Sodium alginate (PRONOVA UP MVG, approximate $M_w = 2.7 \times 10^5$ g/mol, G/M ratio: 1.5, FMC Biopolymer, Princeton, NJ) was gamma (γ) irradiated with a cobalt-60 source for 4 h at a γ dose of 5.0 Mrad for faster degradation[19], resulting in alginate with $M_w = 5.3 \times 10^4$ g/mol. Alginate was then covalently modified with G₄RGDSP (Celtex Peptides, Nashville, TN) using standard carbodiimide chemistry.[20] Sodium hyaluronan (approximately 1200–1900 kDa, FMC Biopolymer) was covalently coupled with G₄RGDSP using similar protocols. The resulting RGD-modified polymers were sterile filtered, lyophilized, and stored at -20°C until use. Control groups formed of unmodified polymers were prepared identically but lacking peptide addition.

RGD-alginate and RGD-hyaluronate were reconstituted separately in α -MEM to obtain 2% (w/v) and 1% (w/v) solutions, respectively. Sterile 0.22 μm filtered RGD-alginate solution was mixed with sterile filtered RGD-hyaluronate solution at 9:1 (v/v) ratio with mineralized microspheres (3 mg/mL final concentration). This solution was then mixed with 100 μL MSCs (10×10^6 cells/mL final concentration in α -MEM). Composite gels were ionically crosslinked by adding 50 μL of supersaturated CaSO₄ to 850 μL composite hydrogel mixture and mixed with 100 μL of the cell suspension. The solution was mixed between two 1-mL syringes (Becton-Dickinson, Franklin Lakes, NJ) coupled with a 3-way stopcock syringe connector with Luer-Lok fittings to minimize air bubbles. The mixture was dispensed between sterile parallel glass plates with 1 mm spacers, allowed to gel for 60 min in a standard CO₂ incubator, and circular gel disks were cut with 8 mm biopsy punches, with each gel containing approximately 5×10^5 cells. The osteogenic potential of this system was evaluated *in vitro* upon transferring constructs to 24-well plates and culturing for 1, 7, 14 or 21 days under standard conditions in osteogenic media (α MEM supplemented with 10% FBS, 1% P/S, 10 mM β -glycerophosphate, 50 μg/mL ascorbate-2-phosphate, 10 nM dexamethasone), which was replaced every 2–3 days.

2.4. Measurement of hydrogel biophysical properties

Covalent modification was confirmed by NMR.[17] ¹H NMR spectra were recorded at 800 MHz using D₂O as a solvent with an NMR spectrometer (Bruker Avance 600). The concentration of RGD conjugated to alginate and hyaluronate was determined using the LavaPep Fluorescent Protein and Peptide Quantification Kit per the manufacturer's instructions (Gel Company, San Francisco, CA). The morphological characteristics of cells seeded in composite mineralized microsphere-loaded hydrogels were observed by scanning

electron microscopy (Philips XL30 TMP field emission SEM, FEI Company, Eindhoven, Netherlands).

Acellular composite hydrogels were prepared as described above, and gels (5 mm diameter and 2 mm height thickness) were cut from a hydrogel sheet and allowed to equilibrate in DI water for 24 h before use. To measure the swelling potential, equilibrated gel samples were weighed, lyophilized for 48 h, and weighed again. The swelling ratio, Q , was determined by calculating the ratio of the equilibrated hydrogel weight to its dry weight ($n=3$ for all samples). Hydrogel dry mass was measured from MSC-loaded hydrogels cultured for up to 28 days in osteogenic media that were lyophilized for 48 h before weighing with a microbalance.

The compressive modulus of composite hydrogels was determined using an Instron 3345 compressive testing system (Norwood, MA). Gels were equilibrated in PBS for 24 h at room temperature prior to measurement. Excess fluid was blotted from the gel surface and then loaded between two flat platens. Hydrogel disks were compressed with a 10 N load cell at 1 mm/min. The compressive elastic modulus, defined as the slope of the linear region of the stress-strain curve of a material under compression, was calculated from the initial linear portion of the curve (0–5% strain, $n=5$ for all groups).[21]

2.5. MSC viability and spreading

MSC-loaded composite gels were rinsed with PBS, minced with a scalpel, homogenized, and collected in passive lysis buffer (Promega). Immediately following one freeze-thaw cycle, lysates were sonicated briefly, centrifuged for 5 min at 10,000 rpm, and the supernatant was used to determine DNA content and intracellular alkaline phosphatase activity (ALP). Total DNA present in each hydrogel construct was quantified using the Quant-iT PicoGreen dsDNA kit (Invitrogen) in comparison to a known standard curve. The remaining homogenized gels were then incubated overnight in H_2SO_4 to solubilize surface calcium deposits. ALP activity and total calcium within composite hydrogels was determined using a *p*-nitrophenyl phosphate (PNPP) colorimetric assay at 405 nm and *o*-cresolphthalein colorimetric assay, respectively.[17] Calcium in acellular gels was quantified and subtracted at each time point to account for calcium present in the mineralized microspheres. After 21 days, some gels were paraffin-embedded, sectioned at 5 μ m, and stained with hematoxylin and eosin (H&E) to assess microsphere morphology and distribution or immunostained for osteocalcin (ab13420, 1:200; Abcam, Cambridge, MA). Viability was assessed *via* the live/dead assay (Invitrogen) and visualized with confocal microscopy on Day 1 and 7 of culture.

2.6. Ovine iliac crest bone defect model

Bilateral critical-sized iliac crest bone defects were surgically created in 12 adult female Swiss Alpine sheep as previously described[22] (Supplementary Figure 1B-I). Animals received preoperative intramuscular antibiotics (naxcel, 2.2 mg/kg) and analgesia (banamine, 1.1 mg/kg) prior to induction of anesthesia. After aseptic preparation and draping, a 10 cm incision was made over the dorsal aspect of each iliac wing. Bilateral full-thickness defects were created in the iliac crest (15 mm diameter, 5 mm depth) using a 15 mm drill bit and

custom-made jig fixed in position using locating screws to ensure the correct location. Approximately 1 mL hydrogel was injected in the defect core using a 21g needle. Three groups were studied (n=5–6 per group): 1) untreated bone defects (sham/empty); 2) acellular composite hydrogels formed of RGD-alginate/RGD-hyaluronate with biomineralized microspheres; or 3) autologous MSCs (10×10^6 cells/mL) delivered in composite hydrogels with biomineralized microspheres. Groups were assigned to the right and left iliac wings to evenly distribute pairs of groups and obtain a balanced experimental design. The periosteum, muscle, and skin were sutured over the iliac crest in layers immediately after the defect filling. After surgery, the animals were allowed to recover and move freely. Animals received an intramuscular injection of banamine (1.0–2.2 mg/kg) postoperatively once a day for 5 days and then as needed for pain control.

2.7. Assessment of bone healing

Radiographs of the sheep ilium were taken at 12 weeks after the surgery to qualitatively assess bone regeneration, while microcomputed tomography (microCT) was performed at 12 weeks from bone explants to quantitatively evaluate bone healing. The original defect site was harvested by collecting a 20 mm diameter and 5–13 mm long bone core cylinder, fixed in formalin overnight and moved to 70% ethanol, and samples with a 15 mm region of interest (ROI) were imaged at 15 μ m resolution (70 kVp, 114 μ A, 300 ms integration time, average of 3 images) using a high-resolution microCT scanner (μ CT 35, Scanco Medical; Brüttisellen, Switzerland). Bone tissue in the reconstructed images was determined by thresholding (1913000 mg HA/cc) to partition mineralized tissue from fluid and soft-tissues, and bone volume fraction (BVF) and bone mineral density (BMD) were calculated from the images.

After imaging, scaffolds were demineralized (Calciclear, National Diagnostics) overnight, bisected, paraffin-embedded, and sectioned at 5 μ m for staining with H&E. Vascularization within the defect area was assessed from H&E-stained sections by counting circular structures with well-defined lumens containing erythrocytes at 100X magnification.[23] Blood vessels were quantified from 3 distinct slides of 4 treated iliac crests per group, and the presence of vessels was confirmed by immunostaining for von Willebrand factor (1:200, ab6994; Abcam). Tissue sections were also stained by Masson's trichrome to detect collagen deposition and osteoid as an indicator of new bone formation and Safranin O/Fast green to detect residual hydrogel.

2.8. Statistical analysis

Data are presented as mean \pm standard deviation for at least three replicates. Statistical significance was assessed by Student's t-test, one-way ANOVA followed by a Tukey's post-hoc test for swelling and mechanical testing, or two-way ANOVA with Bonferroni post-hoc testing for calcium and ALP when appropriate. Statistical analysis was performed using GraphPad Prism® 8 analysis software (GraphPad Software, San Diego, CA). *p*-values < 0.05 were considered statistically significant.

3. RESULTS

3.1. Biophysical properties of composite hydrogels are composition dependent

Gross morphological dimensions and swelling ratio of hydrogels were similar, regardless of composition (Fig. 1A, 1E). RGD conjugation was more efficient on alginate than on hyaluronate, demonstrated by a significant reduction (~40%) in RGD concentration on the backbone of hyaluronate gels (Fig. 1B). RGD conjugation to alginate and hyaluronate was verified by ¹H NMR, which detected characteristic proton peaks at 2.8 and 3.2 ppm for aspartic acid and arginine, respectively (Fig. 1C-D). Pure polymers did not exhibit the presence of these peaks. The addition of hyaluronate, regardless of RGD modification, significantly reduced the compressive modulus compared to RGD-alginate gels alone (Fig. 1F). Quantification of degradation of MSC-containing hydrogels *in vitro* demonstrated a rapid mass loss over the first 7 days in culture that remained constant over the remaining 28 days (Supplementary Fig. 3A).

3.2. In vitro osteogenic response of entrapped MSCs

Ovine MSCs exhibited trilineage potential by differentiation toward the osteoblastic, chondrogenic, and adipogenic lineages when maintained in lineage-specific media for 3 weeks (Supplementary Fig. 2A). MSCs also expressed characteristic cell surface markers when analyzed by flow cytometry (CD90+CD105+CD44+CD45-) (Supplementary Fig. 2B).

Intracellular ALP activity was significantly increased for all gels over 3 weeks in culture (Fig. 2A). MSCs entrapped within RGD-alginate/RGD-hyaluronate exhibited the most rapid increase in ALP activity, which was higher than the other groups at day 14 and higher than RGD-alginate/hyaluronate at day 21. MSCs entrapped in RGD-alginate exhibited a significant increase in ALP activity from day 14 and beyond compared to day 1, ultimately reaching a level 80% of MSCs in RGD-alginate/RGD-hyaluronate. MSCs in RGD-alginate/hyaluronate demonstrated a more cyclical ALP expression profile, reaching the highest level at 3 weeks. For calcium deposition, we observed non-significant increases by MSCs in all gels over time (Fig. 2B). MSCs entrapped in RGD-alginate/RGD-hyaluronate gels exhibited the greatest and only statistically significant increase in calcium at week 3. MSCs entrapped in RGD-alginate/RGD-hyaluronate gels secreted nearly 19-fold more calcium at 3 weeks relative to Day 1 values. DNA content, an indicator of cell number, increased in all gels over three weeks, yet we did not observe differences in DNA content after 3 weeks in culture (*data not shown*). Microspheres appeared randomly distributed and could be observed throughout the hydrogels after 21 days in culture (Fig. 2C). Positive staining for osteocalcin further confirmed that entrapped MSCs were undergoing osteogenic differentiation (Fig. 2D). MSCs remained viable and spread in all gels, with apparent increases in spreading by MSCs in RGD-alginate/RGD-hyaluronate hydrogels (Fig. 3A, B). In light of increases in early and late osteogenic markers by MSCs entrapped in RGD-alginate/RGD-hyaluronate hydrogels containing biomineralized microspheres, we selected this single formulation for examination in the ovine iliac crest defect.

3.3. Assessment of iliac crest bone healing

Locating screws were placed adjacent to the defect at the time of surgery to observe repair from a consistent position. New bone formation within the defect was observed in all animals (Fig. 4A). The untreated sheep showed minimal bone formation within the defect, while defects treated with acellular or MSC-containing RGD-alginate/RGD-hyaluronate gels consistently exhibited formation of new tissue.

Bone explants were harvested to assess the extent of new bone formation by microCT (Fig. 4B). Images of the explants confirm more bone formation occurred in acellular and MSC-loaded composite hydrogels compared to untreated defects. When quantified, we detected significant increases in bone volume fraction for defects treated with MSC-containing composite gels compared to acellular hydrogels or sham-treated defects (Fig. 4C). Bone volume fraction within the defect was similar for sham and acellular hydrogel-treated defects. Similar trends were observed when quantifying bone mineral density (BMD) in the bone defects (Fig. 4D).

Tissue formation was further evaluated by histological evaluation of 12-week tissue explants. We detected significant increases in vascular density of defects treated with MSC-laden constructs compared to acellular gels or sham-treated defects (Fig. 5A, 5B). Clear differences in tissue formation were evident between treatment groups following H&E (Fig. 5C) and trichrome staining (Fig. 5D) when evaluating the entire defect site, with numerous visible areas of osteoid and dense connective tissue.

Higher magnification images of the explants confirmed increased tissue formation and osteoid staining in MSC-loaded hydrogels compared to control or sham defects (Fig. 5D). Collagen fibers, visualized in blue by Masson's trichrome staining, were apparent in all explants. Osteoid formation (dark pink staining) was strongly evident in MSC-laden hydrogels, while more dense, organized tissue was appreciated in defects treated with acellular hydrogels compared to sham controls. Residual hydrogel was not detected in either acellular and MSC-loaded composite hydrogels, as indicated by Safranin O/Fast green staining (Supplementary Fig. 3B), and we observed no histological evidence of a persistent inflammatory response.

4. DISCUSSION

Cell-based approaches to bone healing require the transplantation of cells in carriers that instruct desired cell fate and integrate with surrounding tissues. Hydrogels are ideal vehicles for cell transplantation due to their hydrated nature, tunability, and capacity to gel slowly in order to support cell survival. However, few hydrogels possess the necessary osteoconductive characteristics required to integrate with host bone and nucleate cell-secreted calcium in order to accelerate bone formation. The goal of this study was to test the hypothesis that supplementation of a composite hydrogel with biomineralized substrata would enhance hydrogel osteoconductivity, promote osteogenic differentiation of MSCs, and enhance bone formation in an ovine iliac crest bone defect.

Herein, we describe the development and characterization of composite hydrogels formed of RGD-modified alginate and hyaluronate and containing apatite-coated polymeric microspheres. The swelling ratio, an indicator of the capacity of hydrogels to imbibe water, was not affected by the addition of hyaluronate to alginate hydrogels. However, we detected a significant decrease in the elastic modulus of alginate gels upon addition of hyaluronate. Bone-associated therapies often require stiffer materials, and hydrogels possessing greater elastic moduli are effective for inducing MSCs towards the osteoblastic lineage.[24,25] However, the addition of hyaluronate to this system compensated for the slight reduction in modulus through its other chemical properties that promote osteogenesis. While degradation and associated reductions in mechanical properties were evident after 7 days, we observed a stable and even small increase in dry weight of the hydrogel after 28 days, suggesting that cells were depositing new ECM that compensated for hydrogel degradation.

The hydrophilic nature of alginate does not permit protein adsorption or cell adhesion and requires the covalent incorporation and presentation of adhesion ligands such as RGD. The RGD sequence is the cell attachment site of a large number of adhesive extracellular matrix and cell surface proteins, and nearly half of the over 20 known integrins recognize this sequence in their adhesion protein ligands.[26] RGD modification of hyaluronate was less efficient than alginate (~40%), making the total RGD concentration inconsistent and representing a limitation of our study. However, the small overall volume contribution of hyaluronate used in the composite gel represents a relatively small difference in overall RGD content. Using covalently crosslinked polyethylene glycol hydrogels, increases in RGD concentration correlated with increases in MSC osteogenic differentiation.[27] Similar results were reported for murine and human MSCs in covalently crosslinked alginate gels.[28] However, the gels studied herein were ionically crosslinked and possess dynamic mechanical properties that cells sense, together with ligand concentration, to undergo osteogenic differentiation.[29] When studying ionically crosslinked alginate gels, adhesion and cell proliferation were increased with increasing RGD concentration, but the dose dependence of osteogenic differentiation on RGD concentration was not reported[30]. In this study, we observed increased osteogenic differentiation in composite gels presenting similar RGD concentrations but weaker mechanical properties, further strengthening the beneficial role of hyaluronate in this system. Collectively, this suggests that differences in osteogenesis are derived from other aspects of the composite hydrogel.

Hyaluronate can also function as a cell adhesion molecule, and CD44 can participate in hyaluronate recognition.[31] CD44 is a cluster of differentiation protein commonly used to identify MSCs[16] and enables MSCs to adhere to hyaluronate. Flow cytometry confirmed that ovine MSCs express CD44, providing an additional opportunity for entrapped MSCs to engage both polymers in the composite gel. However, outside of CD44, hyaluronate is unable to engage other cell receptors or integrins, severely limiting its ability to promote adhesion and enable mechanotransduction to regulate MSC phenotype. To enhance adhesivity in composite gels, we covalently modified both polymers with RGD. Robust cell spreading and viability by MSCs in these composite gels, together with increases in early and late osteogenic markers by ovine MSCs, demonstrate the cooperative effects of integrin and CD44 engagement and are in agreement with other studies using RGD-modified hyaluronate gels.[32,33] We hypothesize that MSCs bind to both polymers more uniformly

when entrapped in RGD-alginate/RGD-hyaluronate compared to RGD-alginate/hyaluronate (Fig. 6). The composite gel was ionically crosslinked using divalent calcium ions, physically entrapping the hyaluronate within the crosslinked alginate network. The long-term stability of hyaluronate within this composite hydrogel is unknown and represents an area of future investigation.

To enhance the limited osteoconductivity of this hydrogel formulation, we incorporated polymer microspheres coated with bone-like mineral within the hydrogel to act as a calcium nucleation site. Coating of synthetic polymers such as PLG with carbonated apatite alters cell spreading in 2D[34] and enhances osteoconductivity in 3D porous scaffolds[35]. The addition of mineralized microspheres facilitates a more homogenous distribution of osteoconductive material within the hydrogel compared to pure ceramics that partition rapidly due to differences in density. Biom mineralized microspheres were previously added to fibrin hydrogels to enhance osteoconductivity, evidenced by significant increases in both calcium and phosphate over 3 weeks when entrapped with human MSCs.[14] In this study, the incorporation of RGD- hyaluronate into the composite hydrogel significantly increased early and late markers of osteogenic differentiation by MSCs *in vitro* compared to RGD-alginate/hyaluronate or RGD-alginate alone. These data are in good agreement with the response of human MSCs to fibrin gels containing biom mineralized microspheres[14] and provide a more tunable platform for use in the development of injectable biomaterials for cell transplantation.

The translation of effective tissue engineering approaches for bone healing toward human patients requires their examination in large animal models.[36] In this study, we selected an ovine model of bone healing due to its specific advantages over other large animal models such as the iliac bone dimensions, ease of handling, and calm nature. The site of the bone defect in the iliac crest is effectively non-load bearing, potentially limiting the characterization of bone healing in this model. Bone defects treated with acellular or MSC-laden composite gels were filled with densely packed, cellular and mineralized tissue. We previously studied the capacity of acellular osteoconductive fibrin gels, formed by the incorporation of biom mineralized microspheres, to promote healing of a rat critical-sized calvarial bone defect.[14] Acellular biom mineralized microsphere-loaded fibrin gels did not increase bone formation compared to fibrin gels without microspheres, demonstrating that biom mineralized microspheres are ineffective without the co-transplantation of MSCs. Compared to acellular composite gels in this iliac crest bone defect, we observed significantly greater bone volume in defects treated with MSC-laden composite gels. The treatment of bone defects with acellular composite gels did not yield significant increases in bone volume compared to untreated defects. We are unable to discern whether transplanted autologous MSCs differentiated to osteoblasts to contribute directly to bone formation, or if they induced the migration and differentiation of host progenitor cells and osteoblasts to repair the defect through the MSC secretome. Importantly, none of the animals exhibited a sustained inflammatory response to the material, demonstrating its safety for use in this model. However, bridging was incomplete at 12 weeks, suggesting that additional time is necessary to fully heal this defect.

The formation of a functional vasculature plays a pivotal role in skeletal development and bone repair, and inadequate vascularization delays bone graft regeneration.[37] Implantation of MSCs for bone formation exhibited increased vascularization compared to acellular implants or sham-treated animals[38–40], confirming the proangiogenic potential of MSCs. Although we did not explicitly characterize the secretome of ovine MSCs, numerous studies have reported increased vascularization of defect sites treated with MSCs from various species, and the paracrine effects of MSCs are an important contribution of these cells in tissue regeneration. Defects treated with acellular hydrogels had similar vascular densities as untreated defects, suggesting that the hydrogel alone possesses little proangiogenic potential. Osteoid was evident in defects treated with both acellular or MSC-containing hydrogels, further demonstrating the osteoconductive nature of these composite hydrogels. Defects treated with MSC-laden hydrogels contained substantially more osteoid than acellular hydrogels or untreated defects. We observed considerably more collagen present in defects treated with MSCs in composite hydrogels versus acellular gels or untreated defects. The collective assessments of radiography, microCT, and histology confirm that MSC-laden composite hydrogels containing biomineralized microspheres accelerate bone formation in this ovine iliac bone defect.

5. CONCLUSION

The results of this study demonstrate, for the first time, that injectable composite hydrogels formed of two natural peptide-modified polymers and containing biomineralized microspheres, possess enhanced osteoconductivity, osteogenic potential, and can speed bone formation in a large preclinical animal model. When used to transplant autologous MSCs, this composite hydrogel significantly enhanced neovascularization and bone formation compared to acellular gels, demonstrating its utility as an injectable cell delivery vehicle. These data also reveal that, despite modest adhesivity of MSCs imparted by hyaluronate in this composite gel, osteogenic differentiation was enhanced by coupling the adhesive RGD tripeptide to its backbone. In light of these findings and its contribution to connective tissue homeostasis, the incorporation of hyaluronate into this osteoconductive hydrogel provides advantages for consideration of future platforms designed to promote bone healing.

Supplementary Material

Refer to Web version on PubMed Central for supplementary material.

7. ACKNOWLEDGEMENTS

Research reported in this publication was supported by the National Institute of Dental and Craniofacial Research of the National Institutes of Health under award number R01DE025899 and a University of California Office of the President Proof of Concept Commercialization Gap Grant (12-PC-247641). MGG was supported by the NSF Graduate Research Fellowship and R01 DE025475. CEV was supported by the National Heart, Lung & Blood Institute T32 Training Program in Basic and Translational Cardiovascular Science (T32HL086350). The content is solely the responsibility of the authors and does not necessarily represent the official views of the National Institutes of Health.

REFERENCES

- [1]. Ma J, Both SK, Yang F, Cui FZ, Pan J, Meijer GJ, Jansen JA, van den Beucken JJ, Concise review: cell-based strategies in bone tissue engineering and regenerative medicine, *Stem Cells Transl Med.* 3 (2014) 98–107. [PubMed: 24300556]
- [2]. Leach JK, Whitehead J, Materials-directed differentiation of mesenchymal stem cells for tissue engineering and regeneration, *ACS Biomater Sci Eng.* 4 (2018) 1115–1127. [PubMed: 30035212]
- [3]. Foyt DA, Norman MDA, Yu TTL, Gentleman E, Exploiting advanced hydrogel technologies to address key challenges in regenerative medicine, *Adv Healthc Mater.* 7 (2018) e1700939. [PubMed: 29316363]
- [4]. Zhang YS, Khademhosseini A, Advances in engineering hydrogels, *Science* (80). 356 (2017) eaaf3627.
- [5]. Marquardt LM, Heilshorn SC, Design of injectable materials to improve stem cell transplantation, *Curr Stem Cell Rep.* 2 (2016) 207–220. [PubMed: 28868235]
- [6]. Hersel U, Dahmen C, Kessler H, RGD modified polymers: biomaterials for stimulated cell adhesion and beyond, *Biomaterials.* 24 (2003) 4385–4415. [PubMed: 12922151]
- [7]. Highley CB, Prestwich GD, Burdick JA, Recent advances in hyaluronic acid hydrogels for biomedical applications, *Curr Opin Biotechnol.* 40 (2016) 35–40. [PubMed: 26930175]
- [8]. Makris EA, Gomoll AH, Malizos KN, Hu JC, Athanasiou KA, Repair and tissue engineering techniques for articular cartilage, *Nat Rev Rheumatol.* 11 (2015) 21–34. [PubMed: 25247412]
- [9]. Park H, Lee KY, Facile control of RGD-alginate/hyaluronate hydrogel formation for cartilage regeneration, *Carbohydr Polym.* 86 (2011) 1107–1112.
- [10]. Park H, Lee HJ, An H, Lee KY, Alginate hydrogels modified with low molecular weight hyaluronate for cartilage regeneration, *Carbohydr Polym.* 162 (2017) 100–107. [PubMed: 28224886]
- [11]. Jongpoiboonkit L, Franklin-Ford T, Murphy WL, Mineral-coated polymer microspheres for controlled protein binding and release, *Adv Mater.* 21 (2009) 1960–1963.
- [12]. Kang SW, Yang HS, Seo SW, Han DK, Kim BS, Apatite-coated poly(lactic-co-glycolic acid) microspheres as an injectable scaffold for bone tissue engineering, *J Biomed Mater Res Part A.* 85a (2008) 747–756.
- [13]. Saito E, Suarez-Gonzalez D, Murphy WL, Hollister SJ, Biomineral coating increases bone formation by ex vivo BMP-7 gene therapy in rapid prototyped poly(L-lactic acid) (PLLA) and poly(epsilon-caprolactone) (PCL) porous scaffolds, *Adv Healthc Mater.* 4 (2015) 621–632. [PubMed: 25515846]
- [14]. Davis HE, Binder BY, Schaefer P, Yakoobinsky DD, Bhat A, Leach JK, Enhancing osteoconductivity of fibrin gels with apatite-coated polymer microspheres, *Tissue Eng Part A.* 19 (2013) 1773–1782. [PubMed: 23560390]
- [15]. Dominici M, Le Blanc K, Mueller I, Slaper-Cortenbach I, Marini F, Krause D, Deans R, Keating A, Prockop D, Horwitz E, Minimal criteria for defining multipotent mesenchymal stromal cells. The International Society for Cellular Therapy position statement, *Cytotherapy.* 8 (2006) 315–317. [PubMed: 16923606]
- [16]. Pittenger MF, Mackay AM, Beck SC, Jaiswal RK, Douglas R, Mosca JD, Moorman MA, Simonetti DW, Craig S, Marshak DR, Multilineage potential of adult human mesenchymal stem cells, *Science* (80). 284 (1999) 143–147.
- [17]. Davis HE, Rao RR, He J, Leach JK, Biomimetic scaffolds fabricated from apatite-coated polymer microspheres, *J Biomed Mater Res A.* 90 (2009) 1021–1031. [PubMed: 18655148]
- [18]. Cohen S, Yoshioka T, Lucarelli M, Hwang LH, Langer R, Controlled delivery systems for proteins based on poly(lactic/glycolic acid) microspheres, *Pharm Res.* 8 (1991) 713–720. [PubMed: 2062800]
- [19]. Boontheekul T, Kong HJ, Mooney DJ, Controlling alginate gel degradation utilizing partial oxidation and bimodal molecular weight distribution, *Biomaterials.* 26 (2005) 2455–2465. [PubMed: 15585248]

- [20]. Ho SS, Keown AT, Addison B, Leach JK, Cell migration and bone formation from mesenchymal stem cell spheroids in alginate hydrogels are regulated by adhesive ligand density, *Biomacromolecules*. 18 (2017) 4331–4340. [PubMed: 29131587]
- [21]. Davis HE, Miller SL, Case EM, Leach JK, Supplementation of fibrin gels with sodium chloride enhances physical properties and ensuing osteogenic response, *Acta Biomater*. 7 (2011) 691–699. [PubMed: 20837168]
- [22]. Lansdowne JL, Devine D, Eberli U, Emans P, Welting TJM, Odekerken JCE, Schiuma D, Thalhauser M, Bouré L, Zeiter S, Characterization of an ovine bilateral critical sized bone defect iliac wing model to examine treatment modalities based on bone tissue engineering, *Biomed Res. Int* (2014).
- [23]. Leu A, Stieger SM, Dayton P, Ferrara KW, Leach JK, Angiogenic response to bioactive glass promotes bone healing in an irradiated calvarial defect, *Tissue Eng Part A*. 15 (2009) 877–885. [PubMed: 18795867]
- [24]. Murphy KC, Hughbanks ML, Binder BYK, Vissers CB, Leach JK, Engineered fibrin gels for parallel stimulation of mesenchymal stem cell proangiogenic and osteogenic Potential, *Ann Biomed Eng*. 43 (2015).
- [25]. Cipitria A, Boettcher K, Schoenhals S, Garske DS, Schmidt-Bleek K, Ellinghaus A, Dienelt A, Peters A, Mehta M, Madl CM, Huebsch N, Mooney DJ, Duda GN, In-situ tissue regeneration through SDF-1 α driven cell recruitment and stiffness-mediated bone regeneration in a critical-sized segmental femoral defect, *Acta Biomater*. 60 (2017) 50–63. [PubMed: 28739546]
- [26]. Ruoslahti E, RGD and other recognition sequences for integrins, *Ann Rev Cell Dev Bi*. 12 (1996) 697–715.
- [27]. Yang F, Williams CG, Wang D, Lee H, Manson PN, Elisseff J, The effect of incorporating RGD adhesive peptide in polyethylene glycol diacrylate hydrogel on osteogenesis of bone marrow stromal cells, *Biomaterials*. 26 (2005) 5991–5998. [PubMed: 15878198]
- [28]. Huebsch N, Arany PR, Mao AS, Shvartsman D, Ali OA, Bencherif SA, Rivera-Feliciano J, Mooney DJ, Harnessing traction-mediated manipulation of the cell/matrix interface to control stem-cell fate, *Nat Mater*. 9 (2010) 518–526. [PubMed: 20418863]
- [29]. Chaudhuri O, Gu L, Klumpers D, Darnell M, Bencherif SA, Weaver JC, Huebsch N, Lee HP, Lippens E, Duda GN, Mooney DJ, Hydrogels with tunable stress relaxation regulate stem cell fate and activity, *Nat Mater*. 15 (2016) 326–334. [PubMed: 26618884]
- [30]. Alsberg E, Kong HJ, Hirano Y, Smith MK, Albeiruti A, Mooney DJ, Regulating bone formation via controlled scaffold degradation, *J Dent Res*. 82 (2003) 903–908. [PubMed: 14578503]
- [31]. Peach RJ, Hollenbaugh D, Stamenkovic I, Aruffo A, Identification of hyaluronic acid binding sites in the extracellular domain of CD44, *J Cell Biol*. 122 (1993) 257–264. [PubMed: 8314845]
- [32]. Xiao WK, Zhang RY, Sohrabi A, Ehsanipour A, Sun SP, Liang J, Walthers CM, Ta L, Nathanson DA, Seidlits SK, Brain-mimetic 3D culture platforms allow investigation of cooperative effects of extracellular matrix features on therapeutic resistance in glioblastoma, *Cancer Res*. 78 (2018) 1358–1370. [PubMed: 29282221]
- [33]. Cosgrove BD, Mui KL, Driscoll TP, Caliar SR, Mehta KD, Assoian RK, Burdick JA, Mauck RL, N-cadherin adhesive interactions modulate matrix mechanosensing and fate commitment of mesenchymal stem cells, *Nat Mater*. 15 (2016) 1297–1306. [PubMed: 27525568]
- [34]. Rao RR, He J, Leach JK, Biom mineralized composite substrates increase gene expression with nonviral delivery, *J Biomed Mater Res A*. 94 (2010). doi:10.1002/jbm.a.32690.
- [35]. Murphy WL, Simmons CA, Kaigler D, Mooney DJ, Bone regeneration via a mineral substrate and induced angiogenesis, *J Dent Res*. 83 (2004) 204–210. [PubMed: 14981120]
- [36]. Berner A, Reichert JC, Muller MB, Zellner J, Pfeifer C, Dienstknecht T, Nerlich M, Sommerville S, Dickinson IC, Schutz MA, Fuchtmeier B, Treatment of long bone defects and non-unions: from research to clinical practice, *Cell Tissue Res*. 347 (2012) 501–519. [PubMed: 21574059]
- [37]. Stegen S, van Gestel N, Carmeliet G, Bringing new life to damaged bone: the importance of angiogenesis in bone repair and regeneration, *Bone*. 70 (2015) 19–27. [PubMed: 25263520]
- [38]. Murphy KC, Hughbanks ML, Binder BY, Vissers CB, Leach JK, Engineered fibrin gels for parallel stimulation of mesenchymal stem cell proangiogenic and osteogenic potential, *Ann Biomed Eng*. 43 (2015) 2010–2021. [PubMed: 25527322]

- [39]. Mitra D, Whitehead J, Yasui OW, Leach JK, Bioreactor culture duration of engineered constructs influences bone formation by mesenchymal stem cells, *Biomaterials*. 146 (2017) 29–39. [PubMed: 28898756]
- [40]. Wang L, Fan H, Zhang ZY, Lou AJ, Pei GX, Jiang S, Mu TW, Qin JJ, Chen SY, Jin D, Osteogenesis and angiogenesis of tissue-engineered bone constructed by prevascularized β -tricalcium phosphate scaffold and mesenchymal stem cells, *Biomaterials*. 31 (2010) 9452–9461. [PubMed: 20869769]

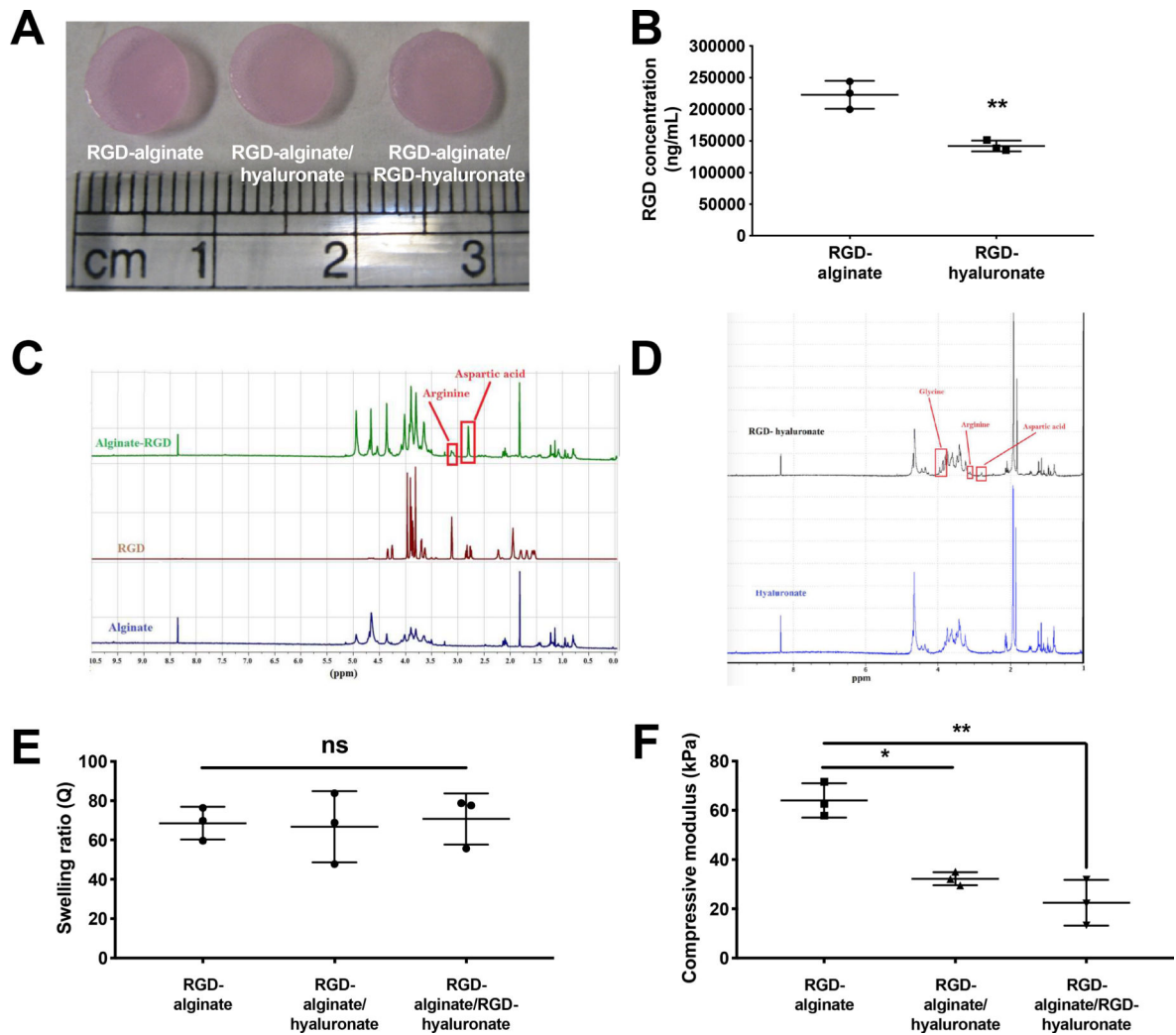


Figure 1. Morphologic and mechanical characterization of composite hydrogels formed of alginate, hyaluronate, and biomaterialized microspheres. (A) Macroscopic morphology of ionically crosslinked cellular hydrogel disks in culture medium after 24 h. (B) Quantification of RGD concentration in RGD-alginate or RGD-hyaluronate (n=3; ** $p < 0.01$). ¹H NMR spectra of RGD-modified (C) alginate and (D) hyaluronate. (E) Swelling ratio in deionized water and (F) compressive moduli (* $p < 0.05$, ** $p < 0.01$; n=3).

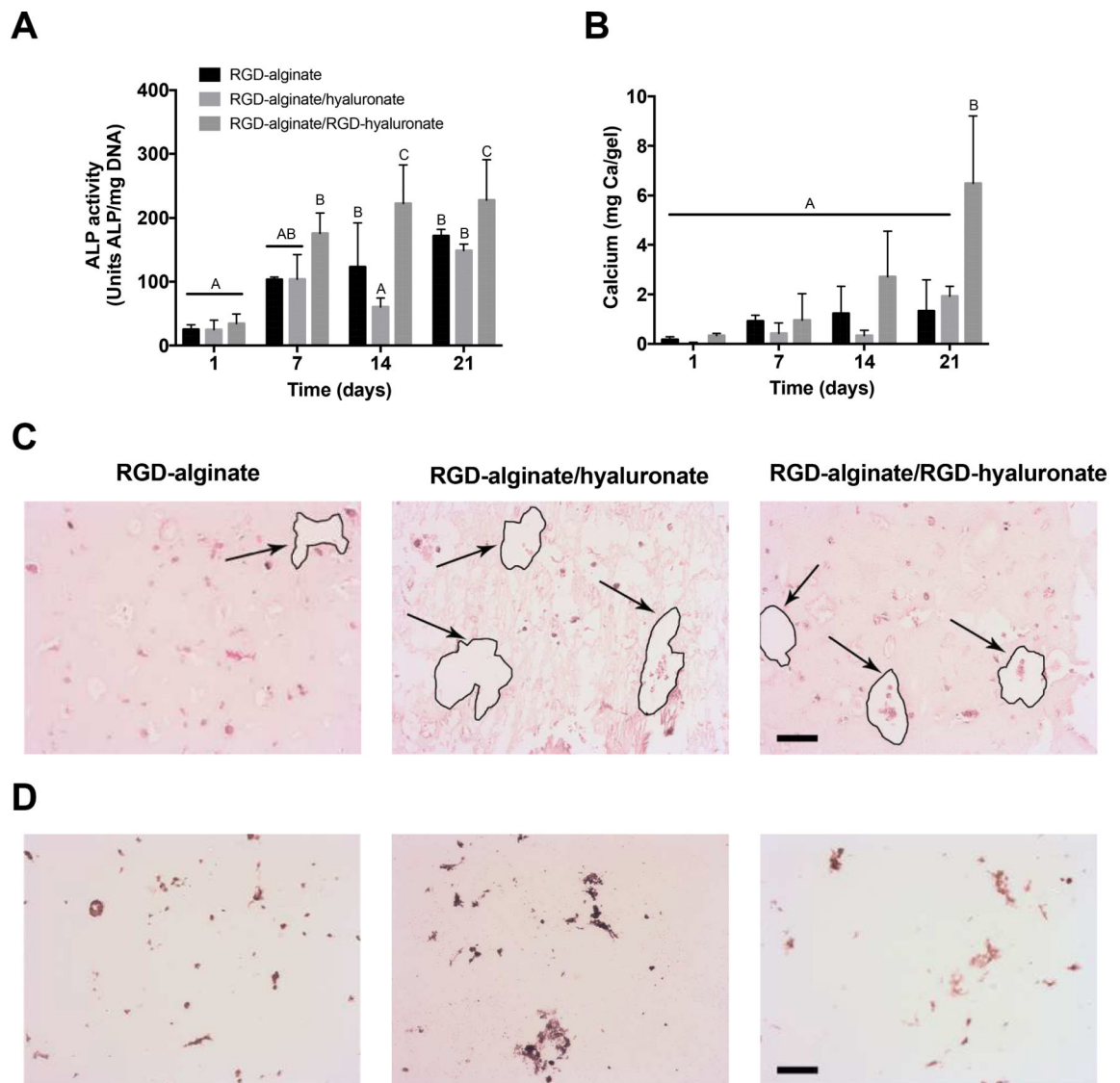


Figure 2. Quantification of *in vitro* osteogenic potential.

(A) ALP activity and (B) total calcium deposition by ovine MSCs entrapped in RGD-alginate, RGD-alginate/hyaluronate, and RGD-alginate/RGD-hyaluronate composite gels over 3 weeks (n=3 for ALP activity, n=4 for total calcium; bars that are statistically different from one another do not share a letter). (C) H&E and (D) osteocalcin staining of gels after 21 days in culture. Arrows and outlines denote location and shape of microspheres, respectively. Scale bar = 50 μ m.

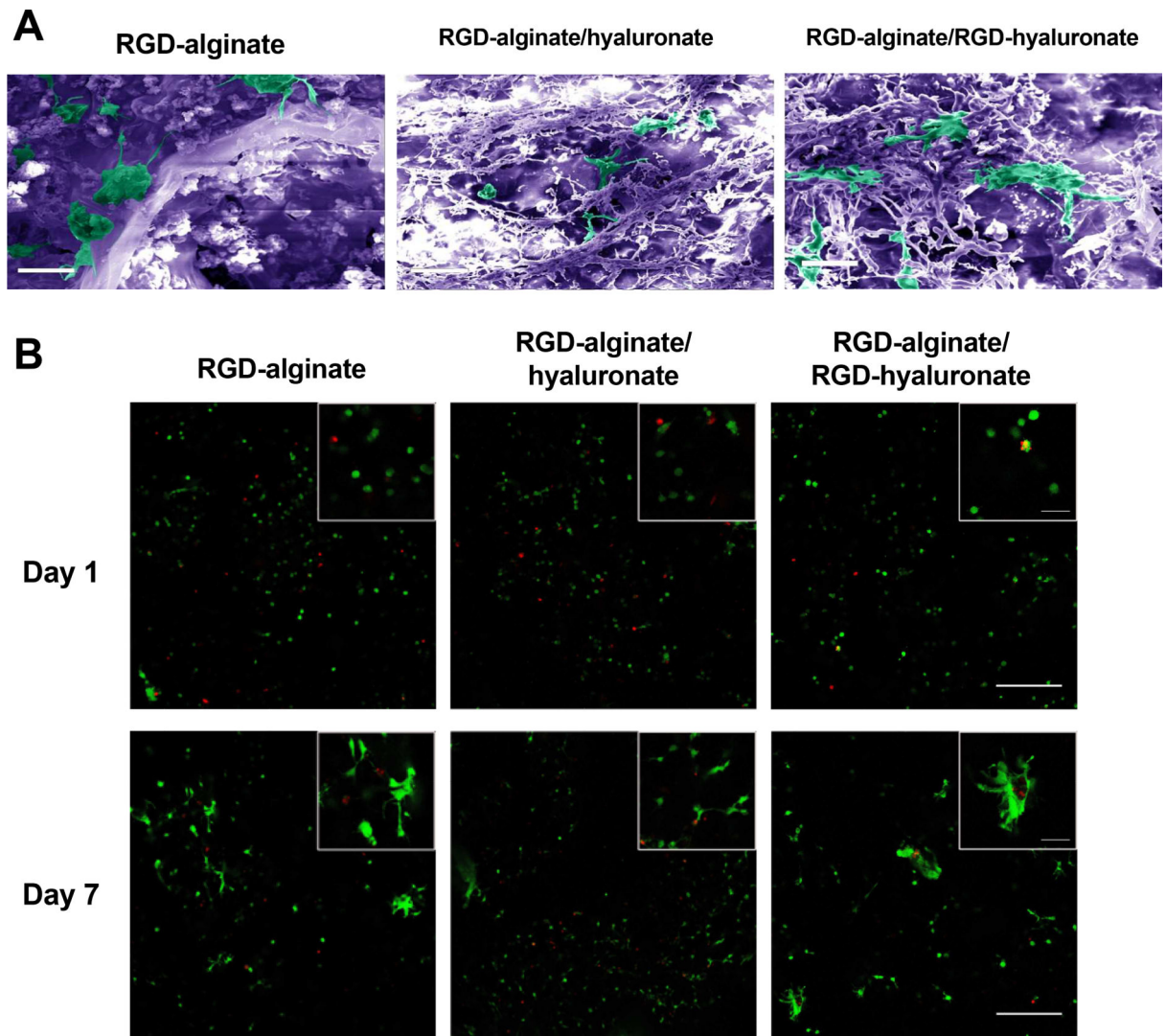


Figure 3. Ovine MSCs spread and are viable in composite hydrogels

(A) False-colored SEM images of MSCs in RGD-alginate, RGD-alginate/hyaluronate, and RGD-alginate/RGD-hyaluronate composite hydrogels (150X) after 21 days in culture. Ovine MSCs are highlighted in green, while purple indicates hydrogel scaffold. Scale bar = 100 μm . (B) Live/dead staining of MSCs entrapped in RGD-alginate, RGD-alginate/hyaluronate, and RGD-alginate/RGD-hyaluronate composite gels over 7 days visualized by confocal microscopy reveal increased spreading in RGD-alginate and RGD-alginate/RGD-hyaluronate at 7 days. Scale bars of original images and inserts are 250 and 50 μm , respectively.

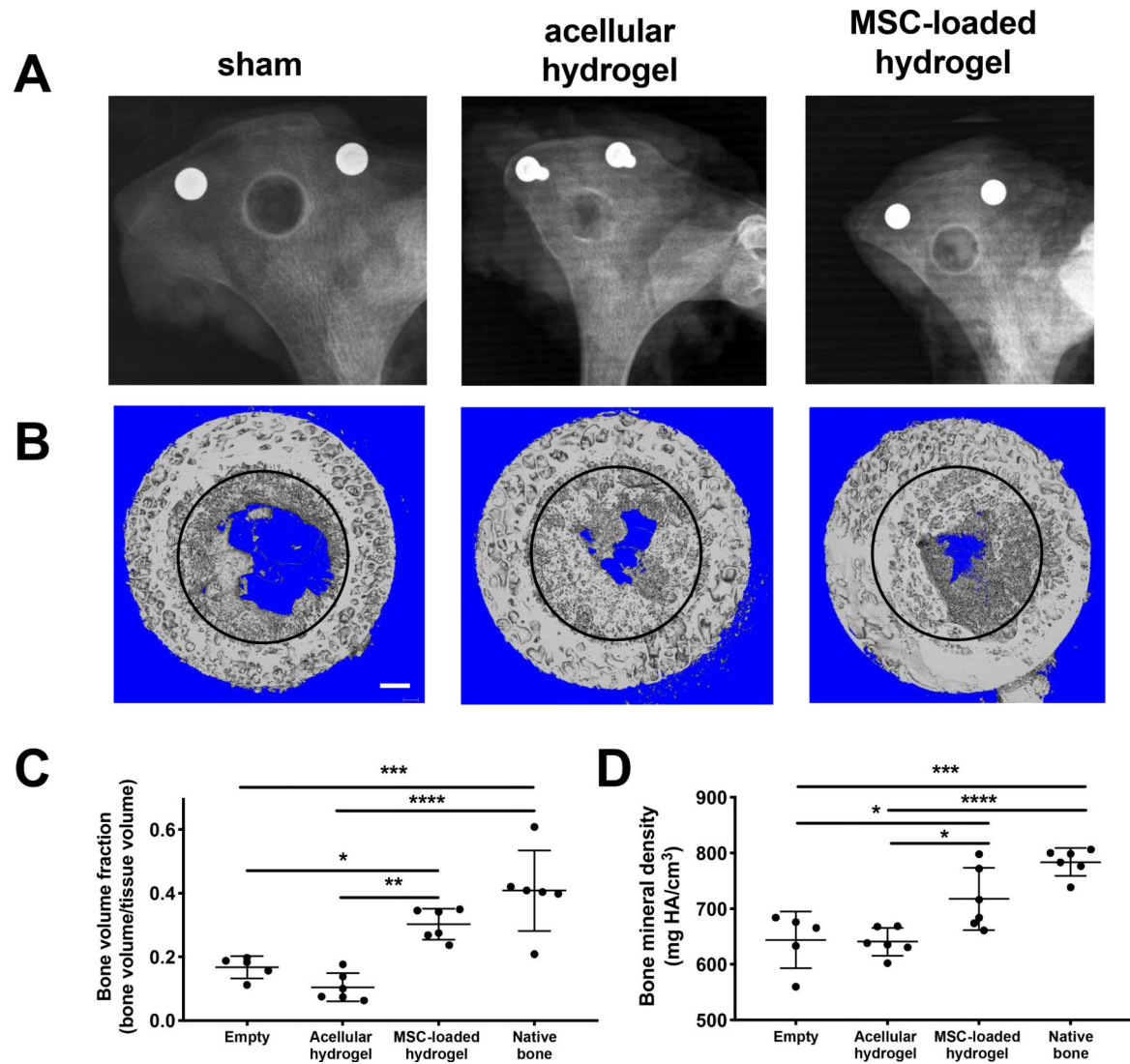


Figure 4. Bone formation in iliac crest defects is increased with MSC-laden composite hydrogels. (A) Representative radiographs of the ovine iliac crest *in vivo* when left untreated (sham) or treated with acellular or MSC-containing RGD-alginate/RGD-hyaluronate composite hydrogels. (B) Representative high resolution microCT images of explants at 12 weeks. Circles denote repair tissue within the 15 mm surgical defect. Scale bar = 2 mm. (C) Bone volume fraction and (D) bone mineral density within the tissue defects (N=5–6 per group). * $p < 0.05$, ** $p < 0.01$, *** $p < 0.001$, **** $p < 0.0001$.

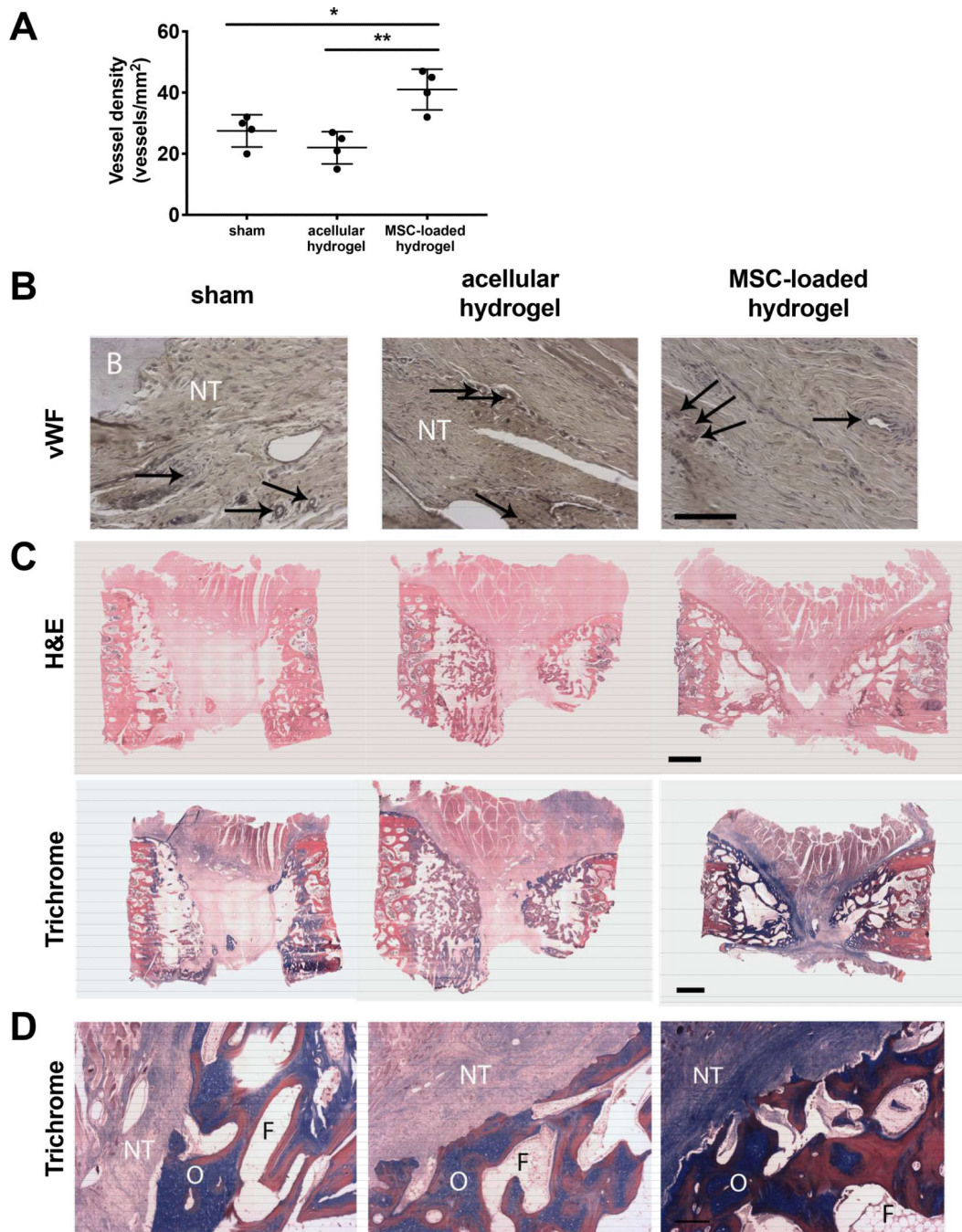


Figure 5. Tissue formation is enhanced with MSC-loaded composite hydrogels.

(A) Quantification of vessel density within repair tissue at 12 weeks (N=4, * $p < 0.05$, ** $p < 0.01$). (B) Representative vWF staining of explants at 20X magnification. Arrows denote vessels; scale bar = 100 μ m. (C) Representative H&E (top) and Masson's trichrome staining (bottom) of entire explants in cross-section. Osteoid is visible in dark pink, collagen fibers are stained blue, and native bone tissue is visible in red. Scale bar = 5 mm. (D) Higher magnification of Masson's trichrome-stained sections. B= bone, O = osteoid, F = fat, NT = new tissue. Scale bar = 100 μ m.

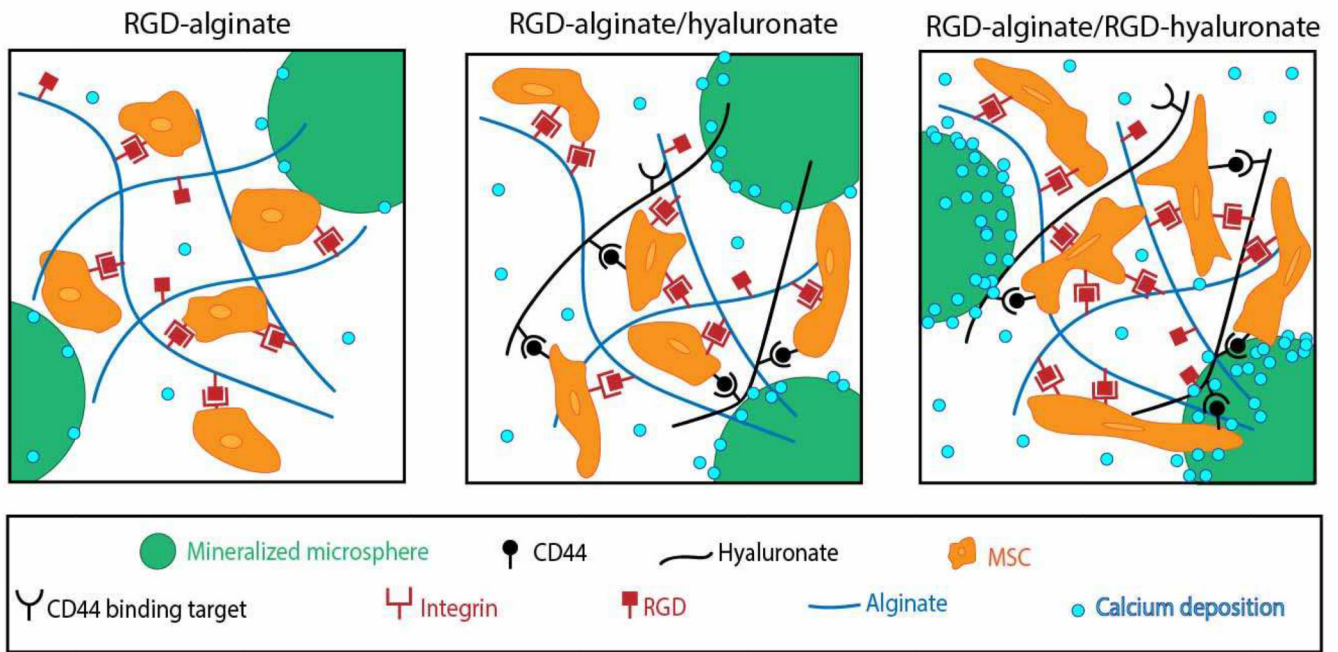


Figure 6. Proposed interaction of MSCs with RGD-alginate/RGD-hyaluronate composite hydrogels.

MSCs engage the RGD adhesive motif on both polymers using various integrins, while also binding to hyaluronate using CD44. MSCs secrete calcium, which is nucleated by entrapped biomineralized microspheres, thereby enhancing hydrogel osteoconductivity and resultant bone formation.